Acknowledgment

References

[1]Na, S. S., and Librescu, L., "Optimal Vibration Control of a Thin-Walled Anisotropic Cantilevers Exposed to Blast Loadings," *Journal of Guidance, Control, and Dynamics*, Vol. 23, No. 3, 2000, pp. 491–500.

[2]Bruch, J. C., Jr., Sloss, J. M., Adali, S., and Sadek, I. S., "Modified Bang–Bang Piezoelectric Control of Vibrating Beams," *Smart Materials and Structures*, Vol. 8, 1999, pp. 647–653.

[3]Song, O., and Librescu, L., "Bending Vibration of Cantilevered Thin-Walled Beams Subjected to Time-Dependent External Excitations," *Journal of the Acoustical Society of America*, Vol. 98, No. 1, 1995, pp. 313–319.

[4]Librescu, L, Song, O., and Rogers, C. A., "Adaptive Vibrational Behavior of Cantilevered Structures Modeled as Composite Thin-Walled Beams," *International Journal of Engineering Science*, Vol. 31, No. 5, 1993, pp. 775–792.

[5]Librescu, L., Meirovitch, L., and Na, S. S., "Control of Cantilevers Vibration via Structural Tailoring and Adaptive Materials," *AIAA Journal*, Vol. 35, No. 8, 1997, pp. 1309–1315.

[6]Wu, Z., and Soong, T. T., "Modified Bang–Bang Control Law for Structural Control Implementations," *Journal of Engineering Mechanics*, Vol. 122, No. 8, 1996, pp. 771–777.

C. Pierre
Associate Editor

Experimental Verification of the Mach-Number Field in a Supersonic Ludwieg Tube

M. Y. El-Naggar,[*] J. T. Klamo,[*] M.-H. Tan,[†]
and H. G. Hornung[‡]
*California Institute of Technology,
Pasadena, California 91125*

I. Introduction

A NEW supersonic Ludwieg tube (LT) was completed at the California Institute of Technology (Caltech) in 2000. A LT, first proposed by Hubert Ludwieg in 1955 in response to a competition (see also Ludwieg et al.[1]), is a blowdown wind tunnel in which the high-pressure reservoir is a long tube. The flow is started by rupturing a diaphragm. The advantage of the long high-pressure reservoir is that, during the time it takes for the expansion wave generated by diaphragm rupture to propagate to the far end of the tube and for its reflection to come back to the diaphragm station, a perfectly uniform reservoir devoid of wave reflections is available to drive a supersonic nozzle. In the Caltech LT, the diaphragm station is located downstream of the nozzle to permit a smooth transition from the tube to the nozzle. Also, the boundary layer developing in the long tube is sucked off through an annular throat just upstream of the nozzle entrance, so that a clean flow is generated. The 300-mm-diam

[*]Graduate Student, Mechanical Engineering, MC 104-44, 1200 E. California Boulevard.

[†]Graduate Student, Graduate Aeronautical Laboratories, 1200 E. California Boulevard.

[‡]C. L. "Kelly" Johnson Professor of Aeronautics, Graduate Aeronautical Laboratories, 1200 E. California Boulevard. Lifetime Fellow AIAA.

tube is 17 m long, the nozzle was designed for a Mach number of 2.3 by J. J. Korte of NASA Langley Research Center, and the test section cross section is 200×200 mm. The useful test time is 75 ms. The aim of the present work was to determine the detailed Mach-number and flow-direction fields by using the method of visualization of Mach waves that was first used by Meyer.[2]

II. Mach-Wave Method

In a steady supersonic flow, disturbances that cause flow deflections generate shock or expansion waves. If the disturbance is infinitesimally small, the wave generated makes an angle μ to the flow that is given by

$$\sin \mu = 1/M \qquad (1)$$

where M is the local Mach number. If two disturbances generate waves that intersect at a point in the flowfield, the local streamline direction bisects the angle made by the two waves, and the latter is therefore 2μ. If sufficiently weak waves can be generated in an experimental flow so that their intersection angle approximates this value closely, visualization of the waves can be used to determine both the local flow direction and the Mach number.

The method is particularly useful in plane flow because weak plane waves are very easily detectable by line-of-sight integrating methods such as schlieren or shadowgraph techniques. The two-dimensional nozzle of the LT is thus an ideal candidate for the method. The sensitivity of the method can be obtained by differentiating Eq. (1):

$$\frac{\mathrm{d}\mu}{\mathrm{d}M} = -\frac{1}{M\sqrt{M^2 - 1}} \qquad (2)$$

showing that it is infinitely sensitive at $M = 1$ and has zero sensitivity at $M = \infty$. At $M = 2.3$ a change of Mach number by 0.01 causes a change of μ of 0.12 deg. The accuracy of the method depends on how weak detectable waves can be made and how accurately the wave angles can be measured. In the Mach-number range of the flow studied here (≤ 2.3) the numbers look promising.

To get a rough idea of how small the strength of the wave has to be for the wave angle to be close enough to μ, an inviscid computation of supersonic flow over a disturbance such as a strip of adhesive tape was made. The result of this computation is shown in Fig. 1. The calculation shows the characteristic divergence of the leading and trailing shock waves. According to weak shock theory,[3] these two shocks lie on a curve of the form

$$y = \left(x / \sqrt{M^2 - 1}\right) \pm a\sqrt{x} \qquad (3)$$

where a is a constant that depends on the obstacle shape. Thus, these two shocks give a very good measure of the Mach angle only in the very far field. In the physical flow, the disturbances are generated by strips of adhesive tape stuck to the top and bottom walls of the nozzle. They are only 0.1 mm thick and are therefore embedded in the nozzle–wall boundary layer and see a flow at a Mach number much smaller than 2.3, so that the waves they generate are much weaker than those in the inviscid computation. This is the reason for our choice of the wedge-shaped leading edge in the computation. Two other features of the flow are the expansion fans from the leading and trailing shoulders of the obstacle. Two straight lines are drawn in the figure at the Mach angle, approximately from the two shoulders. As may be seen, the leading characteristic from the trailing shoulder is almost immediately parallel to the line.

For the computation, the software system Amrita, constructed by J. Quirk,[4] was used. Amrita is a system that automates and packages computational tasks in such a way that the packages can be combined (dynamically linked) according to instructions written in a high-level scripting language. The present application uses features of Amrita that include the automatic construction of an Euler solver, automatic adaptive mesh refinement according to simply chosen criteria, and scripting-language-driven computation and postprocessing of the results. The Euler solver generated for the present computation was an operator-split scheme with HLLE flux and kappa-MUSCL reconstruction. The computation is made with a 90×60
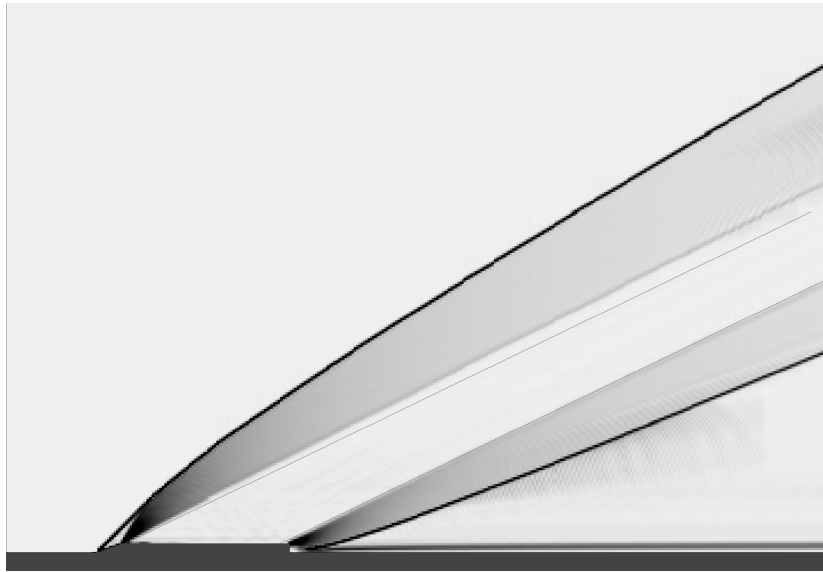
Fig. 1   Pseudoschlieren image of the computation of flow over a disturbance similar to a strip of adhesive tape. Note the divergence of the leading and trailing shocks. The two straight lines are drawn at the Mach angle, and it can be seen that the leading characteristic of the trailing expansion wave is almost immediately parallel to the straight line, whereas the other features are clearly still far from it at 40 disturbance thicknesses downstream.
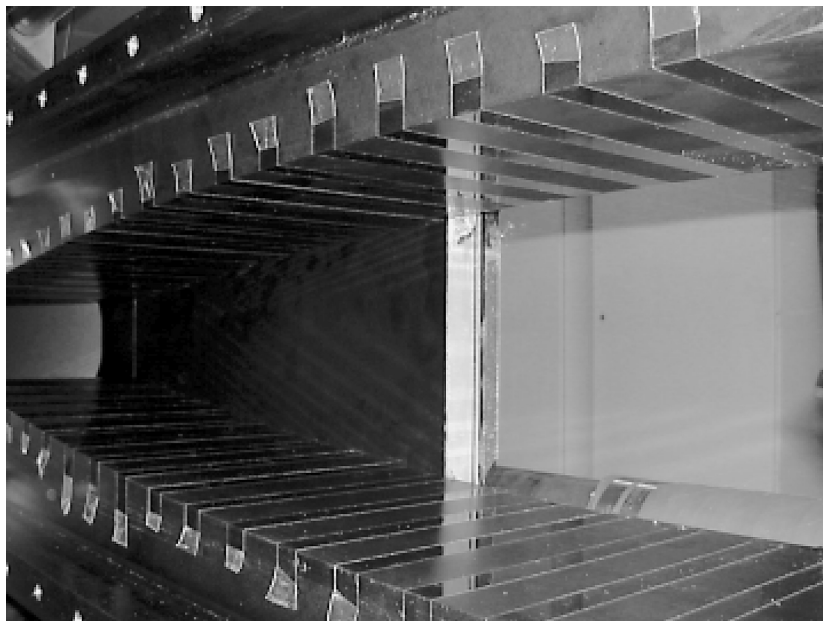

Fig. 2   View of the nozzle with the windows removed, showing the adhesive strips on the top and bottom nozzle walls.

coarse grid, to which three levels of adaptive mesh refinement by a factor of 3 are applied, making the effective grid 810×540.

III.   Results

The optical access to the test section and nozzle of the LT is almost complete; that is, the whole nozzle can be viewed from just downstream of the throat to the end of the test section, including the top and bottom boundary layers. This makes it particularly convenient to use the Mach-wave method to measure the Mach-number distribution in the whole nozzle.

The disturbances are generated by placing equally spaced strips of adhesive tape at right angles to the flow on the top and bottom walls of the nozzle (Fig. 2). The waves generated by the adhesive strips are then visualized by using the schlieren technique. The schlieren system has an aperture of 250 mm, so that, even at the test-section end of the nozzle, where the height of the flow is 200 mm, top and bottom walls can be seen in the same image. By moving the windows and the schlieren system, a composite view of the whole nozzle can

be assembled from several runs of the LT. Such a composite schlieren picture of the nozzle flow is shown in Fig. 3.

As can be seen in Fig. 3, the leading and trailing shocks off the adhesive tape diverge significantly at the upstream end of the nozzle, where the boundary layer is thin. A second reason for the divergence in the upstream region is that the axial Mach-number gradient is quite large there. The divergence decreases rapidly farther downstream as the boundary-layer thickness increases and the Mach-number gradient decreases. The boundary layer can be seen in parts of the picture. Note how, at the downstream end, the curvature of the Mach waves in the boundary layer can clearly be seen.

Figure 4 shows the centerline Mach-number distribution obtained from measurements of the intersection angle of the waves, and Fig. 5 is a plot of the flow angle at a number of transverse cuts along the nozzle.

The Mach-number distribution was also measured by using the centerline pitot-pressure distribution and the wall static-pressure distribution. However, with the pressure transducers used for this
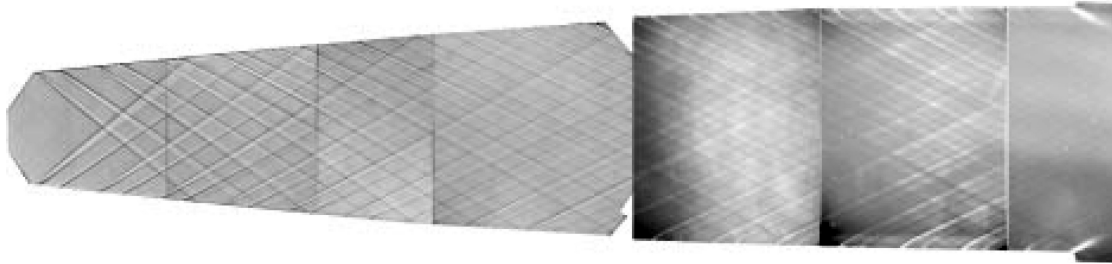
Fig. 3   Composite schlieren picture of the whole nozzle flow, made up of seven separate images. At the upstream end, the leading and trailing shocks diverge significantly. However, farther downstream, where the axial Mach-number gradient is smaller and the boundary layer is thicker, the divergence disappears.
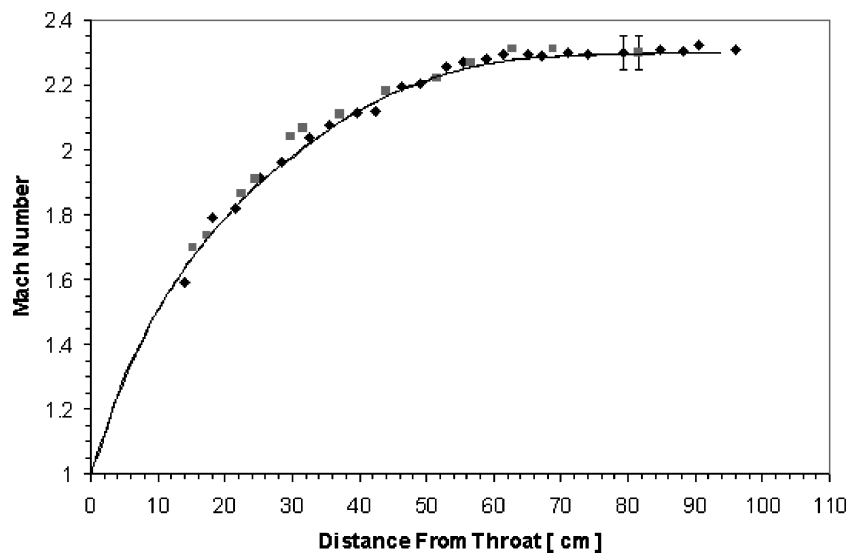

Fig. 4   Mach-number distribution obtained from measurements of the intersection angles of the waves in Fig. 3. The diamonds represent measurements of the intersection of the weak shocks. The squares represent measurements from intersections of the leading characteristics of the trailing expansion waves. The full line is the centerline Mach-number distribution obtained by Korte in his design of this nozzle, which takes account of the boundary-layer displacement thickness.
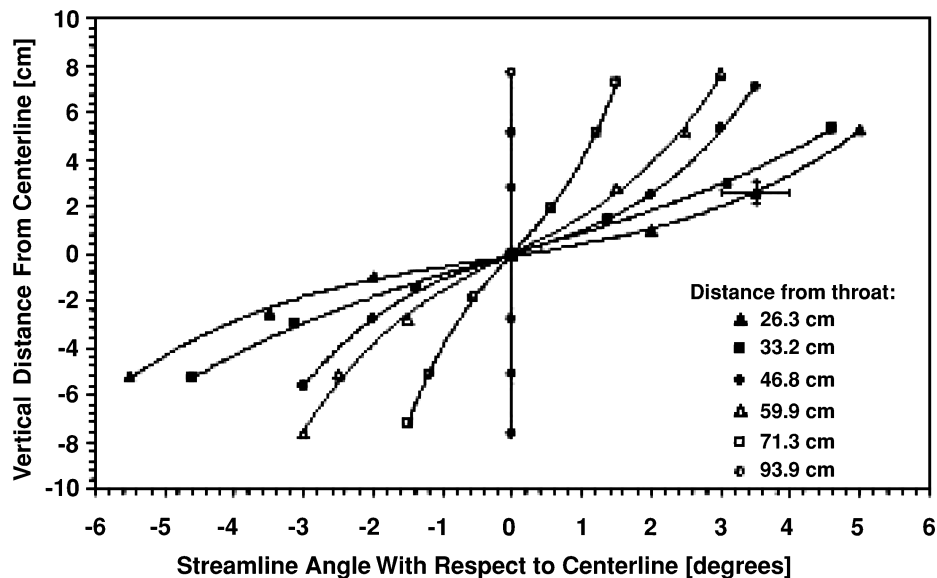

Fig. 5   Plot of the streamline angle against transverse distance at several streamwise stations. To within the accuracy of the method, the flow angle at the last station is zero; that is, the flow in the test section is parallel. The full lines are curves fitted to the experimental points.

purpose, the accuracy of the Mach-wave method was far superior to that of the pressure technique.

IV.   Conclusions

The Mach-number distribution in the Mach 2.3 nozzle of the new Ludwieg tube at the California Institute of Technology has been measured using the Mach-wave intersection method. The centerline Mach-number distribution agrees very well with the design curve, and the flow in the test section is parallel to within the accuracy of the method. The Mach number in the test section is 2.30 ± 0.03. The Ludwieg tube principle is very well suited to university research because of the low cost of operation and the clean flow it provides.

Acknowledgments

References

[1]Ludwieg, H., Hottner, T., and Grauer-Carstensen, H., "Der Rohrwindkanal der Aerodynamischen Versuchsanstalt Göttingen," *Jahrbuch 1969 der DGLR*, Deutsche Gesellschaft für Luft- und Raumfahrt, 1969, pp. 52–58.

[2]Meyer, T., "Über zweidimensionale Bewegungsvorgänge in einem Gas, das mit Überschallgeschwindigkeit strömt," Ph.D. Dissertation, Georgia Augusta Univ., Göttingen, Germany, 1908.

[3]Whitham, G. B., *Linear and Nonlinear Waves*, Wiley, New York, 1974.

[4]Quirk, J. J., "Amrita—A Computational Facility (for CFD Modelling)," von Kármán Inst. for Fluid Dynamics, 29th CFD Lecture Series, von Kármán Inst. for Fluid Dynamics, Brussels, 1998.

M. Sichel
Associate Editor

Applicability of a Simple Method for Thermal Postbuckling of Square Plates

G. Venkateswara Rao* and K. Kanaka Raju†
*Vikram Sarabhai Space Center,
Trivandrum 695 022, India*

Nomenclature

a	=	length of the sides of the square plates
D	=	plate flexural rigidity, $Et^3/12(1-v^2)$
E	=	Young's modulus
N	=	uniform biaxial compressive load developed in the square plate due to temperature rise of ΔT
N_{cr}	=	buckling load of the square plate under uniform biaxial compression
N_x, N_y	=	uniform loads on the square plate in the x and y directions
T	=	uniform biaxial tension developed in the square plate
T_x, T_y	=	uniform tensions developed in the square plate in the x and y directions
t	=	thickness of the square plate
u, v	=	in-plane displacements of the square plate in the x and y directions
w	=	lateral displacement
x, y	=	in-plane coordinates (Fig. 1)
α	=	coefficient of linear thermal expansion
β	=	as defined in Eq. (1)
ΔT	=	temperature rise from the stress free temperature of the square plate
δ	=	central deflection of the square plate
λ_L	=	thermal buckling load parameter defined as $N_{cr}a^2/\pi^2 D$
$\lambda_{Nx}, \lambda_{Ny}$	=	nondimensional parameters, defined as $N_x a^2/\pi^2 D$ and $N_y a^2/\pi^2 D$, respectively
λ_{PB}	=	thermal postbuckling parameter
λ_T	=	nondimensional uniform biaxial tension parameter, defined as $Ta^2/\pi^2 D$
$\lambda_{Tx}, \lambda_{Ty}$	=	nondimensional uniform tension parameters, defined as $T_x a^2/\pi^2 D$ and $T_y a^2/\pi^2 D$, respectively
v	=	Poisson's ratio

Introduction

AEROSPACE structural elements such as uniform columns and plates are subjected to severe environmental conditions, including high thermal loads. The low margins of safety involved in their design lead the designers to use the postbuckling strength of the buckling-prone structural elements, wherever possible.

Classical solutions for predicting the postbuckling strength of these structural elements subjected to mechanical loads are presented by Thompson and Hunt[1] and Dym.[2] A similar study, in which these structural elements are subjected to thermal loads (uniform temperature rise from the stress-free condition of the plate), with ends not free to move axially in the case of columns or with restrained in-plane displacements normal to the edges in the case of the square plates (from now on called immovable edges), is presented by the authors,[3,4] using the versatile finite element method and verified by the classical Rayleigh–Ritz method for square plates with all sides simply supported. It is found from these studies that the thermal postbuckling strength of structural elements is an order of magnitude higher than the mechanical postbuckling strength for a given lateral maximum displacement,[4,5] and this fact can be used advantageously in the design of thermal structures. Thus it will be very useful to design engineers if simpler analytical methods are developed to predict the thermal postbuckling behavior of these structural elements.

Recently, the authors have proposed a simple intuitive method for predicting the thermal postbuckling behavior of uniform columns.[6] The method requires only the tension developed in columns with immovable ends because of large deformations and its critical load for given set of boundary conditions. Applicability of a similar method for evaluating the thermal postbuckling of thin isotropic square plates with immovable edges and different transverse boundary conditions is studied in the present Note. It is found that the present simple method is applicable to predicting the thermal postbuckling of square plates with particular sets of boundary condition, where the tensions developed in the plate, because of large deflections, are equal in the x and y directions (Fig. 1). Librescu et al.[7]

*Group Director, Structural Analysis and Testing Group; currently Professor, Department of Mechanical Engineering, Sreenidhi Institute of Science and Technology, Hyderabad 501 301, India; raohyd@hotmail.com.

†Head, Computational Structural Technology Division, Structural Analysis and Testing Group; kanakaraju_k@vssc.org.
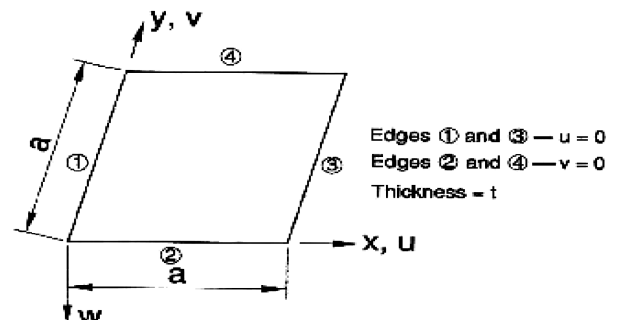

Fig. 1   Square plate with different lateral boundary condition sets on edges 1–4 subjected to uniform thermal load.